The spliceosome inhibitors isoginkgetin and pladienolide B induce ATF3-dependent cell death in mouse embryonic fibroblasts

Erin J. Vanzyl[1] , Hadil Sayed[1] , Alex B. Blackmore[1], Kayleigh R.C. Rick[1], Pasan Fernando[1] and Bruce C. McKay[1,2*]

[1] Department of Biology, Carleton University, Ottawa, ON, Canada

[2]Institute of Biochemistry, Carleton University, Ottawa, ON, Canada

[*] Corresponding author

Email: bruce_mckay@carleton.ca

Abstract

The spliceosome assembles on pre-mRNA in a stepwise manner through five successive pre-spliceosome complexes. The spliceosome functions to remove introns from pre-mRNAs to generate mature mRNAs that encode functional proteins. Many small molecule inhibitors of the spliceosome have been identified and they are cytotoxic. However, little is known about determinants of cell sensitivity. Activating transcription factor 3 (ATF3) is a transcription factor that can stimulate apoptotic cell death in response to a variety of cellular stresses. Here, we used a genetic approach to determine if ATF3 was important in determining the sensitivity of mouse embryonic fibroblasts (MEFs) to two splicing inhibitors: pladienolide B (PB) and isoginkgetin (IGG), that target different pre-spliceosome complexes. These inhibitors led to increased expression of ATF3 in MEFs and importantly, deletion of ATF3 protected MEFs from the cytotoxic effects of these splicing inhibitors, assessed in 3 independent assays. Our results indicate that both splicing inhibitors lead to increased ATF3 expression, and that ATF3 is contributing to the sensitivity of MEFs to these compounds.

Introduction

Most protein-coding genes are transcribed into a precursor RNA (pre-mRNA) that requires significant processing to produce mature mRNA. One of the more complex modifications is the removal of introns and ligation of exons through the process of pre-mRNA splicing [1]. The major spliceosome is responsible for the removal of the vast majority of introns, so it is usually referred to as the spliceosome[1]. The spliceosome is composed of five small nuclear RNAs (snRNAs), U1, U2, U4, U5 and U6, which are each associated with specific proteins yielding their corresponding small nuclear ribonucleoprotein complexes (snRNP). These

snRNPs bind sequentially to *cis*-acting elements in pre-mRNA including the 5' and 3' splice sites, the branch sequence, and polypyrimidine tract, leading to the assembly of a functional spliceosome through the E, A, B, B* and C pre-spliceosome complexes[2].

A variety of small molecules interfere with the spliceosome at distinct points in assembly. PB is a spliceosome inhibitor derived from *Streptomyces platensis* that targets the SF3B1 protein [3]. This protein is a component of the U2 snRNP complex so PB prevents the formation of the A complex [3]. IGG is a natural compound derived from *Ginkgo biloba*, that affects the spliceosome at a subsequent step, preventing the transition from the A to the B complex by inhibiting the stable binding of the U4/U5/U6 tri-snRNP complex [4]. These two compounds affect a different stage of spliceosome formation and it is unclear if they induce cytotoxicity through one or more common pathways [5, 6].

Activating transcription factor 3 (ATF3) is a member of the ATF/CREB transcription factor family and is activated in response to a variety of stresses including DNA damage, inflammation, endoplasmic reticulum (ER) stress and oxidative stress [7-10]. ATF3 has been shown to have a variety of functions, one of which is regulating the expression of proapoptotic genes, such as GADD153/CHOP[11]. We sought to determine if ATF3 plays a role in sensitivity to the inhibition of pre-mRNA splicing. Here we report that ATF3 is induced in mouse embryonic fibroblasts (MEFs) and that deletion of ATF3 in MEFs protects cells from the lethal effects of spliceosome inhibitors. This work provides important insight into the genetic basis of cell death induced by spliceosome dysfunction.

Materials and Methods

Cell culture and drug treatment

ATF3$^{+/+}$ and ATF3$^{-/-}$ MEFs were obtained from Dr. Jim Dimitroulakos (Ottawa Hospital Research Institute)(St. Germain *et al.*, 2010) and grown in DMEM High Glucose media (Hyclone, San Angelo) supplemented with 10% fetal calf serum (FBS) (Gibco, ThermoFisher Scientific, Ottawa) and 90units/ml penicillin, 90ug/ml streptomycin (Hyclone). HCT116 cells were obtained from the American Tissue Type Collection (Cat #: CCL-247, Manassas, VA) grown in McCoys media (Hyclone) supplemented with a 3:1 mixture of Newborn Calf Serum (NBCS) (Gibco, Thermo Fisher Scientific) and Fetal Calf Serum (FBS) (Gibco, ThermoFisher Scientific), and 90 units/ml penicillin, 90 ug/ml streptomycin (Hyclone). Cell were seeded at a density of 500,000 cells/ 6cm or 25,000 cells per well of a 96-well plate, 24 hours prior to treatment, depending on the assay. Cells were treated with up to 30 µM IGG (Calbiochem), up to 25nM PB (ChemCruz), 200nM actinomycin D (AD) (Sigma-Aldrich, St. Louis, MO), an equivalent volume of dimethyl sulfoxide (DMSO) as the vehicle control for IGG or left untreated.

Reverse transcription (RT) and real time quantitative polymerase chain reaction (RT-qPCR)

RNA was isolated from ATF3$^{+/+}$ MEFs using the EZ-10 DNAaway RNA Miniprep Kit from Biobasics and the QIAGEN RNeasy mini kit. Isolated RNA was quantified using the DeNovix DS-11 Spectrophotometer (Wilmington, DE). Equal amounts of RNA were converted to cDNA using the High Capacity cDNA Reverse Transcription kit (Applied Biosystems). For human cells, ATF-3 expression was measured using the Hs00231069_m1 TaqMan® Gene Expression Assays (ThermoFisher Scientific) with GAPDH serving as a sample control (Hs02758991_g1). Bioline SensiFAST™ Probe HI-ROX Master Mix (FroggaBio Inc, Toronto, ON) was used. For

mouse cells, ATF3 expression was normalized to the average of both housekeeping genes; β-actin (ACTB) and Peptidylprolyl isomerase A (PPIA) using the following primers (IDT, Coralville, Ia); ATF3 (F-AAGACAGAGTGCCTGCAGAA, R-GTGCCACCTCTGCTTAGCTC), ACTB (F-GATCTGGCACCACACCTTCT, R-GGGGTGTTGAAGGTCTCAAA) and PPIA (F-AGCTCTGAGCACTGGAGAGA , R-GCCAGGACCTGTATGCTTTA) and Bioline SensiFAST™ SYBR® Hi-ROX Kit.

Immunoblotting

Cell monolayers were rinsed with phosphate buffered saline (PBS) pH 7.6 and collected in 300µl of 1% SDS in dH_2O. Samples were sonicated (QSonic, Newton), and protein was quantified using the Bio-Rad Protein Assay (Bio-Rad, Philadelphia). Equal amounts of protein were denatured in NuPAGE™ LDS Sample Buffer and NuPAGE™ Sample Reducing Agent (10X) (ThermoFisher Scientific, Ottawa), heated for 10 minutes at 70˚C and loaded onto NuPAGE 4-12% Bis-Tris gels (Fisher Scientific). Protein was then transferred to a nitrocellulose membrane (Bio-Rad), and transferred proteins were stained using 1mg/ml Ponceau S Red in 1% glacial acetic acid. Membranes were blocked for 30-60 minutes in 5% Milk in Tris Buffered Saline Tween (TBST) pH 7.6 (Tris Buffered Saline, 0.1% Tween 20). Membranes were incubated overnight at 4˚C in primary antibody, anti-ATF-3 (sc-188, Santa Cruz, CA) or anti-beta-actin (A2228, Sigma) diluted 1:200 for ATF3 or 1:1000 for Actin in 0.5% Milk in TBST pH 7.6. Membranes were washed 4x5 min in TBST, then incubated in secondary antibody (HRP-conjugated goat anti-mouse or goat anti-rabbit from Abcam) for 1-2 hours. Membranes were washed 4x5 min in TBST, then incubated for 5 minutes in 600µl of Clarity™ Western ECL

substrate (Bio-Rad), and imaged using the Fusion FX5 gel documentation system (Vilber Lourmat, France).

Flow cytometry

Floating and adherent cells were collected together by centrifugation following trypsin treatment. The supernatant was removed, and the cell pellet was washed twice in PBS, fixed in 1ml ice cold 70% ethanol and stored at -20˚C for a minimum of 30 minutes. Cells were centrifuged, ethanol was then removed, and the pellet was washed twice in PBS and resuspended in 200µl of 20µM Propidium Iodide (PI) stain (Sigma-Aldrich) with 73µM RNaseA (Fisher Scientific). Red fluorescence was measured with a BD Accuri C6 flow cytometer and analyzed using the BD Accuri C6 software.

Cell viability assays

$ATF3^{+/+}$ and $ATF3^{-/-}$ MEFs were seeded in a 96-well plate 24h hours prior to treatment for both cell viability assays. The CellTiter-Glo® Luminescent Cell Viability Assay (Promega, Madison) was used according to manufacturer's instructions to determine ATP content, to estimate cell viability. Briefly, 100µl of media was removed from each well and mixed with an equal volume of CellTiter-Glo Reagent. After 2 minutes of shaking, the samples were incubated at room temperature for 10 minutes and read using the Cytation 5 96 well plate reader (BioTek, Vermont) and Gen5 software (version 2.07.17) at an integration time of 1.0 s per well.

For trypan blue dye exclusion assays, cells were detached using trypsin and 10 ul of trypan blue (0.4% in PBS) was added to each well of the 96-well plate. After two minutes, an aliquot of cells

was transferred to Dual-Chamber cell counting slides (Bio-Rad, Hercules) and read using the Biorad TC20 Automated Cell Counter.

Results

ATF3 is transcriptionally induced and contributes to cell sensitivity in mouse embryonic fibroblasts

Pre-mRNA splicing is essential for viability and pre-mRNA splicing inhibitors are cytotoxic through an unknown mechanism. It was recently reported that IGG-induces ATF3 indirectly through ATF4, however it was unclear if ATF3 contributed to cell death [12]. Therefore, we used a simple genetic approach to determine if ATF3 contributes to cell death following spliceosome inhibition using isogenic MEF strains that either expressed or did not express ATF3 ($ATF3^{+/+}$ and $ATF3^{-/-}$ MEFs, respectively). ATF3 mRNA levels increased in the $ATF3^{+/+}$ MEFs in response to PB but not IGG exposure (Fig 1A). ATF3 protein increased in response to both drugs, however we detected a greater increase in response to PB (Fig 1B). As expected, ATF3 was not detected in the $ATF3^{-/-}$ MEFs (Figure 1B). We then assessed sensitivity to apoptosis by one parameter flow cytometric analysis of sub G_1 DNA content in both cell lines following exposure to IGG and PB (Fig. 1B). Both drugs led to an increase in the proportion of cells with less than diploid DNA content, however PB led to a greater increase than IGG (Fig 1C). Importantly, cells deleted of ATF3 were significantly protected from drug-induced apoptosis compared to isogenic controls following exposure to both drugs. Therefore, PB and IGG appear to induce ATF3-dependent apoptosis in MEFs.

Fig 1. ATF3 is activated in response to IGG and PB treatment in MEFs. ATF3$^{+/+}$ and ATF3$^{-/-}$ MEFs were left untreated, or exposed to DMSO, 30μM IGG or 25nM PB for 24 hours. (A) ATF3 mRNA levels were quantified in ATF3+/+ MEFs using qRT-PCR and these were normalized to ACTB and PPIA mRNA levels. (B) Protein lysates were collected in 1% SDS and analyzed using immunoblot with the indicated antibodies. MagicMark™ Western Protein Standard was used, the 30kDa and 40kDa marker are visible on ATF3 and actin westerns, respectively. Similar results were obtained in 4 independent experiments and mean fold change is indicated below each lane of the immunoblot. Flow cytometric analysis of sub G_1 content was completed as described previously for both ATF3$^{+/+}$ and ATF3$^{-/-}$ cells (B). A t-test was completed for each individual treatment to compare cell lines (*$p<0.05$, **$p<0.01$, ***$p<0.001$).

The sensitivity of MEFs to spliceosome inhibition was further evaluated with two additional independent assays. First, ATF3$^{+/+}$ and ATF3$^{-/-}$ MEFs were exposed to either IGG or PB for 24h and cell viability was assessed by trypan blue dye exclusion (Fig 2A). Trypan blue is unable to penetrate viable cells with intact cell membranes, whereas non-viable cells that have lost membrane integrity take up the dye. Both splicing inhibitors (PB and IGG) decreased cell viability in ATF3$^{+/+}$ MEFs. The surviving fractions of ATF3$^{-/-}$ MEFs were significantly higher than parental controls following exposure to both drugs. In fact, there was no detectable decrease in viability in the ATF3$^{-/-}$ MEFs with this assay.

Fig 2. The absence of ATF3 increases cell viability following PB and IGG treatment. ATF3$^{+/+}$ MEFs (white) and ATF3$^{-/-}$ MEFs (grey) were incubated with 30μM IGG, 25nM PB and 200nM act D for 48h (A) or 24h (B). A trypan blue exclusion assay was used to assess

membrane integrity, as an indicator of cell viability (A). The CellTiter-Glo® Luminescent Cell Viability Assay was used to estimate metabolic activity as an indicator of cell viability (B). Each bar represents the mean of 3 independent experiments, +/- SEM. Statistical significance between cell lines for each treatment was completed using a t-test (*$p<0.05$, **$p<0.01$, ***$p<0.001$).

Second, a CellTiter-Glo® Luminescent Cell Viability Assay was used to quantify ATP levels in treated and untreated cells. A decrease in ATP in treated compared to untreated cells is indicative of a decrease in the number of metabolically active cells (Fig 2B). ATP levels decreased in both $ATF3^{+/+}$ and $ATF3^{-/-}$ MEFs following treatment with IGG and PB, however the surviving fraction of treated $ATF3^{-/-}$ MEFs was significantly greater than the surviving fraction of control MEFs. $ATF3^{-/-}$ MEFs were again protected from the cytotoxic effects of both PB and IGG. Taken together, ATF3 expressing MEFs are more sensitive to splicing inhibitors than their $ATF3^{-/-}$ counterparts, as assed by DNA fragmentation, membrane integrity and ATP content. ATF3 is important in multiple cell death pathways [7, 11, 13] but its contribution to cell sensitivity to the spliceosome inhibitors was unknown.

Splicing inhibitors induce apoptosis and increase ATF3 in human colon cancer cells

Our results provide compelling genetic evidence that ATF3 contributes to cell death induced by spliceosome inhibitors in MEFs. We sought to determine if splicing inhibitors similarly led to ATF3 induction in human cells. Therefore, we measured the expression of ATF3 mRNA and protein in response to treatment with both splicing inhibitors in HCT116 cells (Fig 3A and B). ATF3 mRNA and protein increased significantly in response to both drugs with a greater fold increase in response to PB (Fig 3A and B). Similarly, HCT116 cancer cells were

exposed to either IGG or PB and 48 hours later apoptosis was assessed by flow cytometric analysis of subG_1 DNA content (Fig 3C and D). Exposure to either splicing inhibitor resulted in an increase in the fraction of cells with sub G_1 DNA content under condition that induced ATF3 expression (Figs 3C and D). These results support the concept that ATF3 is induced upon spliceosome disruption and that this likely contributes to cell death in human cells, as well.

Fig 3. Increased apoptotic cell population in response to IGG and PB treatment. HCT116 cells were left untreated, exposed to 30μM IGG or 25nM PB for 24h (A and B) or 48 hours (C and D). ATF3 levels were measured by qRT-PCR (A) and immunoblotting (B). Flow cytometric analysis was performed to determine the proportion of cells with sub G_1 DNA content (apoptotic) after 48 hours for 30 μM IGG (C) and 25 nM PB (D). Each point in A, C and D) represents the mean, +/- the standard error of the mean (SEM) from at least three independent experiments. Statistical significance was determined using a one-way Anova followed by a Tukey's post-test (*$p<0.05$, **$p<0.01$, ***$p<0.001$). In B, similar results were obtained in three independent experiments and the mean fold change in protein expression is presented below the representative immunoblot.

Discussion

The production of functional mRNAs requires the synthesis of pre-mRNA that is coordinated with co-transcriptional mRNA processing steps including pre-mRNA splicing [14-16]. The inhibition of pre-mRNA splicing delays or prevents the production of functional mRNAs and indirectly the encoded proteins. How splicing abnormalities are sensed and transmitted to cell death pathways remains unclear. In the present work, we measured cellular

responses to two spliceosome inhibitors, IGG and PB. We found that both drugs led to an increase in ATF3 expression in human colon cancer cells and MEFs. Parental MEFs, expressing ATF3, were sensitive to both inhibitors leading to a large decrease in the viable cell population. However, cell viability was significantly higher in ATF3-/-, as assessed in 3 independent assays. Subtle quantitative differences were detected among the assays that reflect the timing of individual assays, the measured characteristic of cell death (DNA fragmentation, loss of membrane integrity or loss of ATP) and the sensitivity of individual assays. The trypan blue exclusion assay required the analysis of cell viability before cell detachment. In addition, CellTiter-Glo® Luminescent Cell Viability Assay is not determined on a single cell basis and it is very sensitive [17] so it isn't entirely surprising that we detected greater apparent cell death with this assay. Despite these differences, all three assays support a model in which ATF3 is a major regulator of mammalian cell sensitivity to these pre-mRNA splicing inhibitors.

The two spliceosome inhibitors tested target distinct pre-spliceosome complexes. PB interacts with the SF3B1 subunit of the U2 snRNP in the complex A [5] whereas IGG acts somewhat later preventing the transition from the A to B complex through an unknown target [4]. Despite the fact that both drugs inhibit pre-mRNA splicing at similar stages and induce apoptosis through an ATF3-dependent mechanism, a variety of differences in gene expression and biological effects have been described. For example, we have previously reported that these two drugs can have pronounced effects on cell cycle distribution but these changes were not identical [18]. Two parameter flow cytometric analysis of bromodeoxyuridine-labelled cells indicated that IGG led to multiple cell cycle alterations but the most prominent was to an S phase arrest [18]. In partial contrast, PB-treated cells were blocked predominantly in G_1 but also exhibited a more modest S phase arrest than IGG-treated cells [18]. Meanwhile, both drugs led

to decreased M phase assessed by loss of phospho-H3 immunoreactivity [18]. Therefore, there are similarities and differences in the effects of these compounds on cell cycle responses.

Other groups have reported recently that IGG has other unique effects on transcription and protein trafficking. Boswell and coworkers found that IGG decreases transcription elongation, in addition to its effects on pre-mRNA splicing [19]. Strand-specific RNA-sequencing (RNA-seq) was performed in IGG-treated and control cells and relative read number increased within 5 kb of transcription start sites in IGG-treated cells but not in the presence of an SF3B1 inhibitor, meayamycin [20], suggesting that transcription near the 5'end of genes was slow in the presence of IGG [19]. These authors also detected increased polyA site readthrough in IGG treated cells further suggesting that a fundamental problem in transcription and co-transcriptional processing may underlie some of the unique biological effects of IGG [19]. It is noteworthy that these authors still detected a defect in pre-mRNA splicing using RNA-seq analysis in this and previous papers [19, 21].

Lastly, IGG also appear to inhibit trafficking of the amyloid precursor protein (APP) from endoplasmic reticulum (ER) to the Golgi [22] and lysosome-mediated turnover [12]. In the former, APP levels increased in response to IGG but not the SF3B1 inhibitor spliceostatin [22]. APP was retained in the ER where the protein was stable and accumulated [22]. In the latter paper [12], IGG led to increased lysosomal stress, increased TFEB protein expression (a regulator of lysosomal biogenesis) and the accumulation of polyubiquitinated proteins under nutrient starving conditions suggesting that IGG may be inhibiting proteasomes and altering lysosomal function under some conditions [12]. Intriguingly, IGG-induced TFEB activated ATF3 indirectly through ATF4, however it was unclear if ATF3 contributed to cell death detected in this manuscript. There is presently no evidence that PB or any other SF3B1 inhibitors

similarly affect protein homeostasis. While these additional functions attributed to IGG may contribute to differences detected in cell cycle regulation [18], they don't appear to strictly alter the ATF3-dependence of cell death induced by IGG and PB. It is likely that IGG and PB lead to ATF3 induction through a common mechanism related to spliceosome inhibition.

Conclusions

ATF3 is involved in a variety of stress pathways, and it is likely that a disruption in spliceosome formation is leading to activation of ATF3, in turn promoting apoptosis. The novel findings here provide evidence that splicing inhibitors lead to activation of ATF3, and that ATF3, in turn, is playing a role in determining sensitivity of cells to these compounds. Our future work will investigate the role ATF3 has on cell sensitivity, and work to determine how each of these splicing inhibitors specifically led to ATF3 activation.

Acknowledgements

We would like to thank Dr. Jim Dimitroulakos (Princess Margaret Research Institute, Toronto, ON) for providing mouse embryonic fibroblasts.

References

1. Hoskins AA, Moore MJ. The spliceosome: a flexible, reversible macromolecular machine. Trends Biochem Sci. 2012;37(5):179-88. doi: 10.1016/j.tibs.2012.02.009. PubMed PMID: 22480731; PubMed Central PMCID: PMCPMC3508674.
2. Jurica MS, Moore MJ. Pre-mRNA splicing: awash in a sea of proteins. Molecular cell. 2003;12(1):5-14. doi: 10.1016/s1097-2765(03)00270-3. PubMed PMID: 12887888.
3. Kotake Y, Sagane K, Owa T, Mimori-Kiyosue Y, Shimizu H, Uesugi M, et al. Splicing factor SF3b as a target of the antitumor natural product pladienolide. Nature chemical biology. 2007;3(9):570-5. PubMed PMID: 17643112.
4. O'Brien K, Matlin AJ, Lowell AM, Moore MJ. The biflavonoid isoginkgetin is a general inhibitor of Pre-mRNA splicing. The Journal of biological chemistry. 2008;283(48):33147-54. PubMed PMID: 18826947.

299 5. Yokoi A, Kotake Y, Takahashi K, Kadowaki T, Matsumoto Y, Minoshima Y, et al. Biological
300 validation that SF3b is a target of the antitumor macrolide pladienolide. FEBS J. 2011;278(24):4870-80.
301 doi: 10.1111/j.1742-4658.2011.08387.x. PubMed PMID: 21981285.
302 6. Yoon SO, Shin S, Lee HJ, Chun HK, Chung AS. Isoginkgetin inhibits tumor cell invasion by
303 regulating phosphatidylinositol 3-kinase/Akt-dependent matrix metalloproteinase-9 expression.
304 Molecular cancer therapeutics. 2006;5(11):2666-75. PubMed PMID: 17121913.
305 7. Fan F, Jin S, Amundson SA, Tong T, Fan W, Zhao H, et al. ATF3 induction following DNA damage
306 is regulated by distinct signaling pathways and over-expression of ATF3 protein suppresses cells growth.
307 Oncogene. 2002;21(49):7488-96. doi: 10.1038/sj.onc.1205896. PubMed PMID: 12386811.
308 8. Gurzov EN, Barthson J, Marhfour I, Ortis F, Naamane N, Igoillo-Esteve M, et al. Pancreatic beta-
309 cells activate a JunB/ATF3-dependent survival pathway during inflammation. Oncogene.
310 2012;31(13):1723-32. doi: 10.1038/onc.2011.353. PubMed PMID: 21841823.
311 9. Schroder M, Kaufman RJ. ER stress and the unfolded protein response. Mutation research.
312 2005;569(1-2):29-63. doi: 10.1016/j.mrfmmm.2004.06.056. PubMed PMID: 15603751.
313 10. Fels DR, Koumenis C. The PERK/eIF2alpha/ATF4 module of the UPR in hypoxia resistance and
314 tumor growth. Cancer Biol Ther. 2006;5(7):723-8. doi: 10.4161/cbt.5.7.2967. PubMed PMID: 16861899.
315 11. Thompson MR, Xu D, Williams BR. ATF3 transcription factor and its emerging roles in immunity
316 and cancer. J Mol Med (Berl). 2009;87(11):1053-60. doi: 10.1007/s00109-009-0520-x. PubMed PMID:
317 19705082; PubMed Central PMCID: PMCPMC2783469.
318 12. Tsalikis J, Abdel-Nour M, Farahvash A, Sorbara MT, Poon S, Philpott DJ, et al. Isoginkgetin, a
319 Natural Biflavonoid Proteasome Inhibitor, Sensitizes Cancer Cells to Apoptosis via Disruption of
320 Lysosomal Homeostasis and Impaired Protein Clearance. Molecular and cellular biology. 2019;39(10).
321 doi: 10.1128/MCB.00489-18. PubMed PMID: 30910794; PubMed Central PMCID: PMCPMC6497994.
322 13. Mungrue IN, Pagnon J, Kohannim O, Gargalovic PS, Lusis AJ. CHAC1/MGC4504 is a novel
323 proapoptotic component of the unfolded protein response, downstream of the ATF4-ATF3-CHOP
324 cascade. J Immunol. 2009;182(1):466-76. PubMed PMID: 19109178; PubMed Central PMCID:
325 PMCPMC2846782.
326 14. Saldi T, Cortazar MA, Sheridan RM, Bentley DL. Coupling of RNA Polymerase II Transcription
327 Elongation with Pre-mRNA Splicing. J Mol Biol. 2016;428(12):2623-35. doi: 10.1016/j.jmb.2016.04.017.
328 PubMed PMID: 27107644; PubMed Central PMCID: PMCPMC4893998.
329 15. Carmo-Fonseca M, Kirchhausen T. The timing of pre-mRNA splicing visualized in real-time.
330 Nucleus. 2014;5(1):11-4. doi: 10.4161/nucl.28056. PubMed PMID: 24637398; PubMed Central PMCID:
331 PMCPMC4028348.
332 16. Lee KM, Tarn WY. Coupling pre-mRNA processing to transcription on the RNA factory assembly
333 line. RNA Biol. 2013;10(3):380-90. doi: 10.4161/rna.23697. PubMed PMID: 23392244; PubMed Central
334 PMCID: PMCPMC3672281.
335 17. Nowak E, Kammerer S, Kupper JH. ATP-based cell viability assay is superior to trypan blue
336 exclusion and XTT assay in measuring cytotoxicity of anticancer drugs Taxol and Imatinib, and
337 proteasome inhibitor MG-132 on human hepatoma cell line HepG2. Clin Hemorheol Microcirc.
338 2018;69(1-2):327-36. doi: 10.3233/CH-189120. PubMed PMID: 29630545.
339 18. Vanzyl EJ, Rick KRC, Blackmore AB, MacFarlane EM, McKay BC. Flow cytometric analysis
340 identifies changes in S and M phases as novel cell cycle alterations induced by the splicing inhibitor
341 isoginkgetin. PLoS One. 2018;13(1):e0191178. doi: 10.1371/journal.pone.0191178. PubMed PMID:
342 29338026; PubMed Central PMCID: PMCPMC5770052.
343 19. Boswell SA, Snavely A, Landry HM, Churchman LS, Gray JM, Springer M. Total RNA-seq to
344 identify pharmacological effects on specific stages of mRNA synthesis. Nature chemical biology.
345 2017;13(5):501-7. doi: 10.1038/nchembio.2317. PubMed PMID: 28263964.

346 20. Albert BJ, McPherson PA, O'Brien K, Czaicki NL, Destefino V, Osman S, et al. Meayamycin inhibits
347 pre-messenger RNA splicing and exhibits picomolar activity against multidrug-resistant cells. Molecular
348 cancer therapeutics. 2009;8(8):2308-18. PubMed PMID: 19671752.
349 21. Gray JM, Harmin DA, Boswell SA, Cloonan N, Mullen TE, Ling JJ, et al. SnapShot-Seq: a method
350 for extracting genome-wide, in vivo mRNA dynamics from a single total RNA sample. PLoS One.
351 2014;9(2):e89673. doi: 10.1371/journal.pone.0089673. PubMed PMID: 24586954; PubMed Central
352 PMCID: PMCPMC3935918.
353 22. Bai B, Wang S, Chen Y, Jia J, Tian X, Liu C, et al. Effects of RNA Splicing Inhibitors on Amyloid
354 Precursor Protein Expression. ACS Omega. 2018;3(3):2798-803. doi: 10.1021/acsomega.7b02073.
355 PubMed PMID: 30221221; PubMed Central PMCID: PMCPMC6130791.

356

A

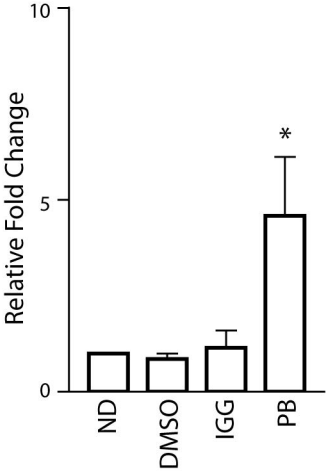
10
5
0
Relative Fold Change
*
ND
DMSO
IGG
PB

B

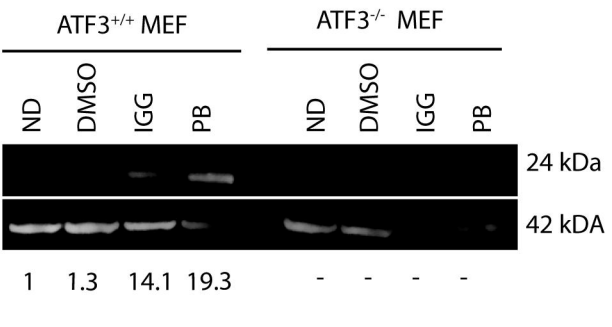
ATF3+/+ MEF
ATF3-/- MEF
ND
DMSO
IGG
PB
ND
DMSO
IGG
PB
ATF3
24 kDa
Actin
42 kDA
Fold change
1
1.3
14.1
19.3
-
-
-
-

C

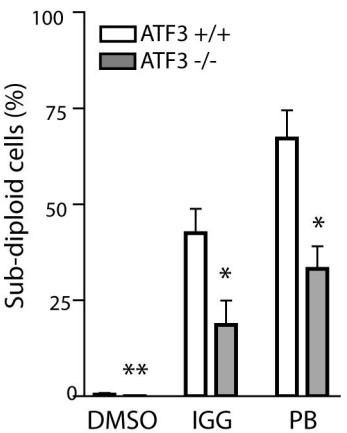
100
75
50
25
0
Sub-diploid cells (%)
ATF3 +/+
ATF3 -/-
**
*
*
DMSO
IGG
PB

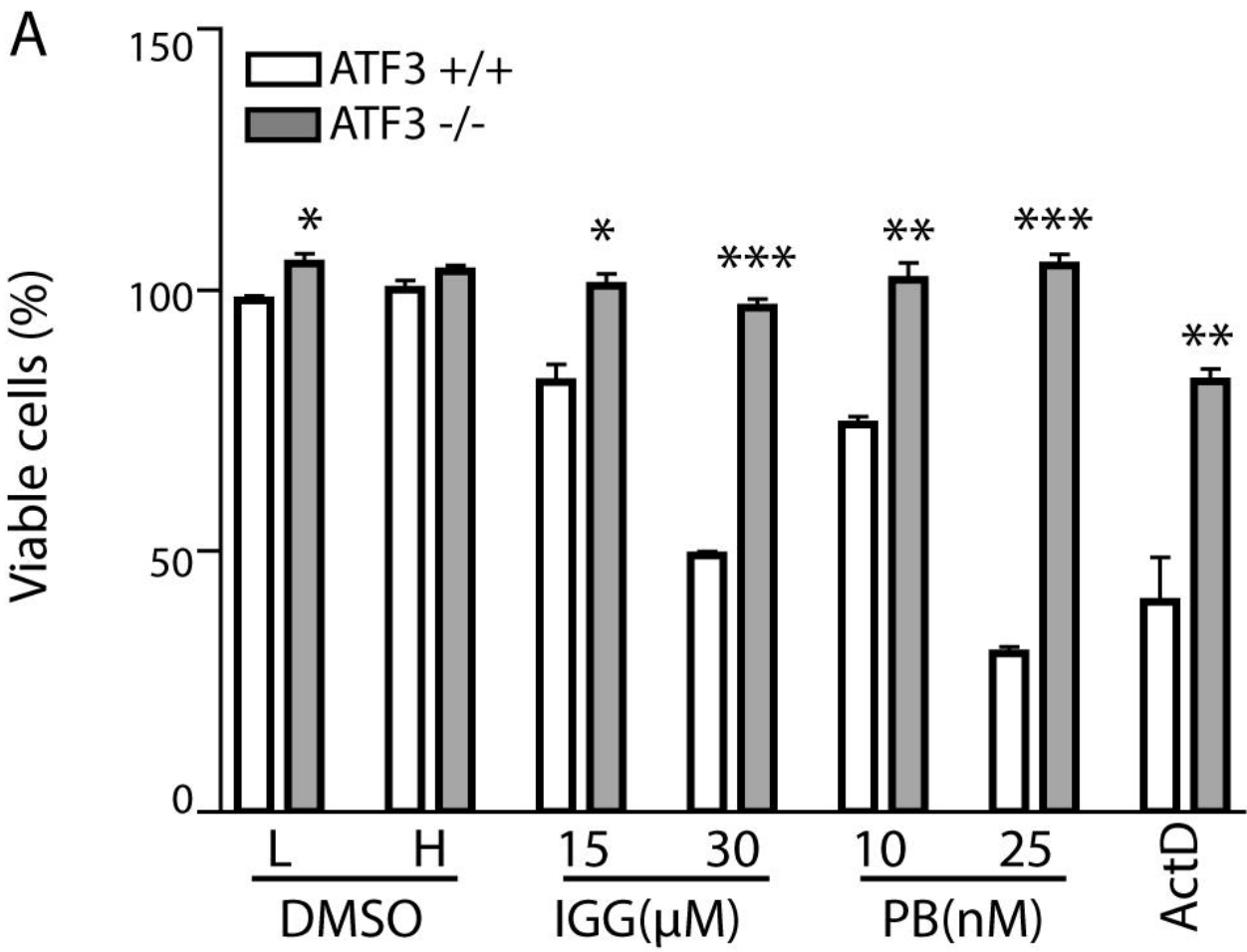
A
ATF3 +/+
ATF3 -/-
Viable cells (%)
150
100
50
0
*
*
***
**
***
**
L
H
15
30
10
25
ActD
DMSO
IGG(μM)
PB(nM)

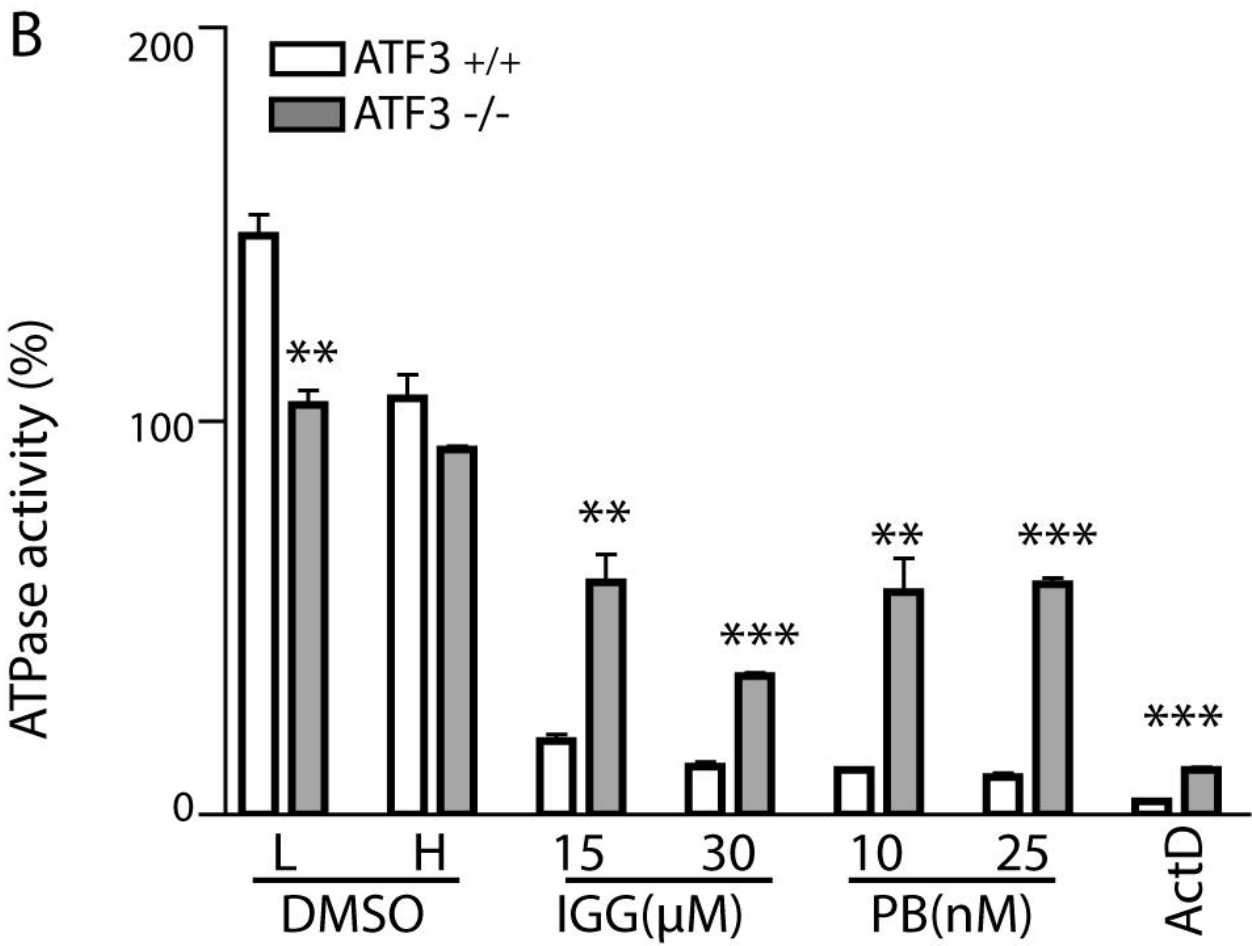
B
ATF3 +/+
ATF3 -/-
ATPase activity (%)
200
100
0
**
**
***
**
***
***
L
H
15
30
10
25
ActD
DMSO
IGG(μM)
PB(nM)

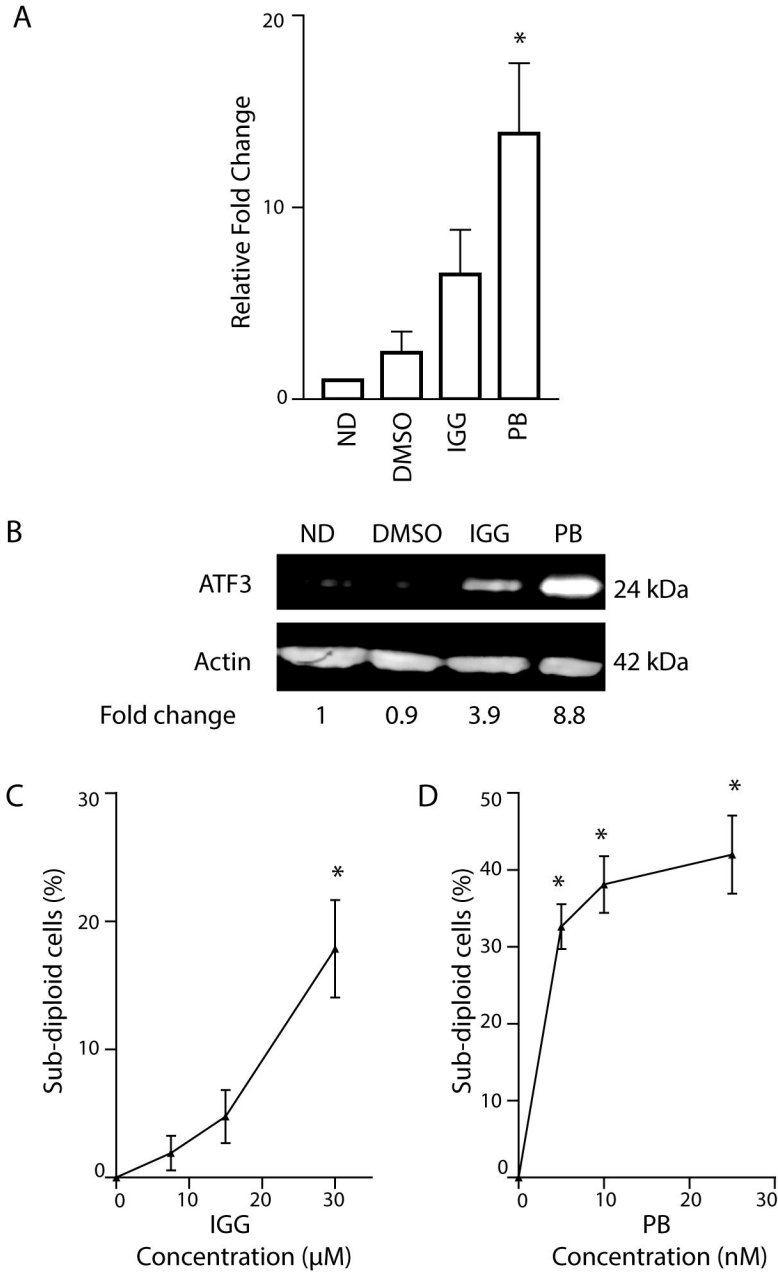
A
Relative Fold Change
20
10
0
*
ND
DMSO
IGG
PB
B
ND
DMSO
IGG
PB
ATF3
24 kDa
Actin
42 kDa
Fold change
1
0.9
3.9
8.8
C
Sub-diploid cells (%)
30
20
10
0
*
0
10
20
30
IGG
Concentration (μM)
D
Sub-diploid cells (%)
50
40
30
20
10
0
*
*
*
0
10
20
30
PB
Concentration (nM)